Bubble-Point Pressures, Saturated- and Compressed-Liquid Densities of the Binary R-125 + R-143a System[1]

T. Fujimine[2,3], H. Sato[2] and K. Watanabe[2]

[1] Paper presented at the 13th Symposium on Thermophysical Properties, June 22-27, 1997, Boulder, Colorado, USA

[2] Department of System Design Engineering, Faculty of Science and Technology, Keio University, 3-14-1, Hiyoshi, Kohoku-ku, Yokohama 223, Japan

[3] To whom correspondence should be addressed.

ABSTRACT

Bubble-point pressures, saturated- and compressed-liquid densities of the binary R-125 (pentafluoroethane)+ R-143a (1,1,1-trifluoroethane) system have been measured for several compositions at temperatures from 280 to 330 K by means of a magnetic densimeter coupled with a variable-volume cell mounted with a metallic-bellows. The experimental uncertainties of the temperature, pressure, density measurements and the composition determination were estimated to be within ± 10 mK, ± 12 kPa, ± 0.2 % and ± 0.2 mass%, respectively. The purity of the samples used throughout the measurements are 99.96 area% for R-125 and 99.94 area% for R-143a. Based on these measurements, the thermodynamic behavior of the vapor-liquid equilibria of this binary refrigerant mixture has been discussed using the Peng-Robinson equation for the bubble-point pressures, and a developed correlation for the saturated-liquid densities and equation of states for the compressed-liquid densities.

KEY WORDS : alternative refrigerant; binary R-125 + R-143a mixtures; bubble-point pressure; compressed-liquid density; R-125, R-143a; saturated-liquid density; vapor-liquid equilibria.

INTRODUCTION

Recent concerns on the research and development of CFC and HCFC alternatives have forced HFC refrigerant mixtures to be considered as perspective replacements for some CFCs and HCFCs.

The nonflammable R-125 and the flammable R-143a both have vapor-pressures similar to those of R-502 (the azeotropic mixture of R-22 and R-115). Therefore, their mixture can be expected as a promising alternative to replace R-502. The present work aims to investigate the bubble-point pressures, the saturated- and compressed-liquid densities of the binary R-125 + R-143a system.

MEASUREMENTS AND RESULT

All measurements in the present work were performed with a magnetic densimeter coupled with a variable volume cell which enables measurements either at the saturated-liquid condition or at the compressed-liquid condition. The apparatus is schematically shown in Fig.1 by which we have performed similar measurements for several alternative refrigerant mixtures [1-3]. The pressure was measured through digital quartz pressure gauge (F, J). The sample density was directly measured by a magnetic densimeter (A), while the temperature was measured by means of a standard platinum resistance thermometer (R) placed in the vicinity of the magnetic densimeter. Controlling the pressure of the nitrogen gas filled in the outer part of the metal bellows allows the sample to be brought into the saturated- and/or compressed-liquid condition. The saturation state of the mixture with known composition was determined by observing the appearance and disappearance of a bubble in the liquid phase. The sample purities analyzed by the chemical manufacturers are 99.96 area% for R-125 and 99.94 area% for R-143a, respectively, and no further purification was performed in the present work. We estimated uncertainties of measurements following the ISO guide [4] on the basis of expanded uncertainty with a coverage factor k = 2. The experimental

uncertainties of the temperature, bubble-point pressure, and density measurements and the composition determination were estimated to be not greater than ±10 mK, ±12 kPa, ± 0.2 %, and ± 0.2 mass%, respectively. The uncertainty in pressure measurements for $P\rho Tx$ properties of compressed liquid was estimated to be within ± 2 kPa, whereas that in The uncertainty in bubble-point pressure measurement becomes ±12 kPa due to possible error in saturation point determination.

We have measured the bubble-point pressures, saturated- and compressed-liquid densities of the binary R-125 + R-143a system for temperatures from 280 to 330 K in 10 K intervals up to 3 MPa and for composition of 0, 20, 40, 50, 60, 80, 100 mass% R-125. The experimental results are summarized in Tables I and II.

DISCUSSION

The Peng-Robinson (PR) equation has been applied to analyze the bubble-point pressures obtained in the present work. The binary interaction parameter, k_{ij}, in this equation has been optimized being k_{ij} = -0.0126 on the basis of the present data and the data by Nagel and Bier [5]. The critical parameters of R-125 and R-143a used throughout the present study are given in Table III. The critical temperature, density and pressure of the binary mixtures of the present interest are those determined by Higashi [6]. The relative deviation of bubble-point pressures from the PR equation at various molar fractions x_1 of R-125 is plotted in Fig. 2. As shown in Fig. 2, the optimized PR equation can reproduce the present data within ± 1 % and most of the reported data agree with the PR equation within ± 2 %. The effective range of the optimized PR equation covers temperatures from 200 to 330 K.

The PR equation, which is widely being employed in industrial applications, is confirmed effective only in reproducing the bubble-point pressures but not the saturated-liquid densities. [7] We applied the new correlation proposed by Widiatmo et al [8] for saturated-liquid densities of mixtures. The correlation is given by Eq. (1).

$$\rho_r = 1 + \mathrm{A_m}\tau^{\mathrm{a_m}} + \mathrm{B_m}\tau^{\mathrm{b_m}} + \mathrm{C_m}\tau^{\mathrm{c_m}} \tag{1}$$

where $\rho_r = \rho/\rho_{\mathrm{cm}}$ and $\tau = 1 - T/T_{\mathrm{cm}}$.

The subscript m denotes mixtures. The loci of the critical temperature, T_{cm}, critical pressure, P_{cm}, and critical density, ρ_{cm}, for the binary R-125 + R-143a system are those optimized by Higashi [6] based on their own measurements. The coefficients $\mathrm{A_m}$, $\mathrm{B_m}$ and exponents $\mathrm{a_m}$, $\mathrm{b_m}$ are representaively given by Eq. (2).

$$\mathrm{Y_m} = \theta_1 \mathrm{Y_1} + (1-\theta_1)\mathrm{Y_2} + \theta_1(1-\theta_1)\mathrm{Y_{12}} \quad (\ \mathrm{Y = A, B, C, a, b, c}\ ) \tag{2}$$

$$\theta_{\mathrm{i}} = \frac{x_{\mathrm{i}} V_{\mathrm{ci}}^{2/3}}{\sum_{\mathrm{j}} x_{\mathrm{j}} V_{\mathrm{cj}}^{2/3}} \tag{3}$$

θ_1 denotes the surface fraction of R-125 defined by Eq.(3). We determined the parameters used in Eq.(2) based on the data by the present work, those by Widiatmo et al. [7] and Ikeda and Higashi [9]. The numerical values of $\mathrm{Y_{12}}$ for the binary R-125 + R-143a system as well as the values of $\mathrm{Y_1}$, $\mathrm{Y_2}$ for pure substances, R-125 and R-143a, are given in Table IV. Figs. 3 and 4 depict the deviation of measured saturated-liquid densities from Eq.(1) which represents the present data within ± 0.2 %. Since most of the reported data agree with Eq.(1) within ± 0.3 %, Eq.(1) seems to be an appropriate saturated-liquid density representation for the binary R-125 + R-143a system. The effective range of Eq.(1) covers temperatures from 280 to 330 K.

Sato [10] proposed an empirical equation to represent the liquid phase $P\rho T$ properties of water, which is given as follows;

$$\rho_r = (P_r + E)^{\mathrm{D}} / \mathrm{F} \tag{4}$$

We have applied this model for representing the present compressed-liquid $P\rho Tx$ properties and saturated-liquid densities of the binary R-125+ R-143a system as follows;

$$\rho_r = (P_r + \mathrm{E_m})^{\mathrm{D_m}} / \mathrm{F_m} \tag{5}$$

where $\rho_r = \rho/\rho_{\mathrm{cm}}$ and $P_r = P/P_{\mathrm{cm}}$.

The subscript m denotes mixtures and the parameters D_m, E_m and F_m are correlated as follows;

$$\mathrm{D_m} = \mathrm{d_1} + \mathrm{d_2}\tau \tag{6}$$

$$\mathrm{E_m} = \mathrm{e_1}\tau + \mathrm{e_2}\tau^2 + \mathrm{e_3}\tau^4 \tag{7}$$

$$\mathrm{F_m} = \mathrm{f_1} + \mathrm{f_2}\tau + \mathrm{f_3}\tau^2 + \mathrm{f_4}\tau^4 \tag{8}$$

where $\tau = 1 - T/T_{\mathrm{cm}}$.

We applied a simple mixing rule for each numerical constant as given in Eq.(9). The data used to determine the parameter values in Eq.(9) are the present saturated- and compressed-liquid densities and those by Widiatmo et al.[7]. The numerical parameter values thus determined are summarized in Table VI.

$$\mathrm{y_i} = x_1\mathrm{y_{i1}} + (1 - x_1)\mathrm{y_{i2}} + x_1(1 - x_1)\mathrm{y_{i3}} \quad (\mathrm{y} = \mathrm{d, e, f}) \tag{9}$$

x_1 denotes molar fraction of R-125. The deviation of liquid densities from Eq.(5) is plotted in Figs. 5 and 6. As shown in Figs. 5 and 6, Most of the present data and the data by Widiatmo et al. [7] agree with Eq.(5) within ± 0.2 %. The effective range of Eq.(5) covers temperatures from 280 to 330 K and pressures up to 3 MPa.

CONCLUSIONS

One-hundred and sixty-eight compressed liquid $P\rho Tx$ properties including essential thermodynamic properties at the two phase condition of the binary R-125 + R-143a system have been measured over range of temperatures 280-330 K, pressures up to

3 MPa at compositions of 0, 20, 40, 50, 60, 80, 100 mass% R-125.

The optimized PR equation can reproduce most of the reported bubble-point pressure data within ± 2 %. The saturated-liquid densities are also well reproduced within ± 0.3 % by the developed correlation for saturated-liquid density. The compressed-liquid $P\rho Tx$ properties are satisfactorily represented by the equation of state we developed within ± 0.2 % in density.

ACKNOWLEDGMENTS

We are indebted to Asahi Glass Co. Ltd., Tokyo and Daikin Industries, Ltd. Osaka for their valuable cooperation in furnishing the research-grade samples of R-125 and R-143a. The assistance by Akina Kozakai is also greatly acknowledged.

REFERENCES

1. Widiatmo, J. V., Sato, H., Watanabe, Fluid Phase Equilibria, 99, 1994, 199.
2. Widiatmo, J. V., Sato, H., Watanabe, Proc. Asia-Pacific Conf. on the Built Environment, 1995, 253
3. Widiatmo, J. V., Sato, H., Watanabe, J. Chem. Eng. Data, 42(2), 1997, 270
4. International Organization for Standardization, “Guide to the Expression of Uncertainty in Measurement”, 1993, Switzerland.
5. Nagel, M., Bier, K., Int. J. Refrigeration, 1995, 18 (8), 264.
6. Higashi, Y., Proc. of the 1996 JAR Annual Conf., 1996, 93 (in Japanese).
7. Widiatmo, J. V., Sato, H., Watanabe, K., Int. J. Thermophys., 1995, 16 (3), 801.
8. Widiatmo, J. V., Sato, H., Watanabe, K., Proc. of the 16th Japan Symp. on Thermophys. Prop. 1995, 181.
9. Ikeda, T., Higashi, Y., Proc. of the 16th Japan Symp. on Thermophys. Prop. 1995, 169 (in Japanese).
10. Sato, H., Ph..D. Dissertation, 1981, Keio University, Yokohama, Japan.
11. Takashima, H., Higashi, Y., Proc. of the 16th Japan Symp. on Thermophys. Prop. 1995, 9. (in Japanese)
12. Zhelezny, V., Chernyak, Y., Zhelezny, P., Proc. of the 4th Asian Thermophys. Prop. Conf., 1995, 327.
13. Kishizawa, G., Sato, H., Watanabe, K., Paper to be presented at the 13th Symp. on Thermophys. Prop., 1997.

FIGURE CAPTIONS

Fig. 1 Experimental apparatus

(A) magnetic densimeter (B) variable volume cell (C) digital quartz pressure transducer (D) damper (E) thermostat (F) digital quartz pressure gauge (G) vacuum pump (H) vacuum gauge (I) nitrogen gas (J) digital quartz pressure computer (K) main heater (L) subheater (M) cooler (N) stirrer (O) standard resistor (P) PID controller (R) standard platinum resistance thermometer (S) pressure gauge (T) digital multimeter (U) current controller (V1-V) valves (W) DC power supply (X) galvanometer (Y) thermometer bridge (Z) pen recorder (Ω) transformer (Φ) personal computer

Fig. 2 Relative deviation of bubble-point pressures at different compositions from the PR equation

Nagel and Bier [5], ¢ Takashima and Higashi [11]
Widiatmo et al. [7], Zhelezny et al. [12], This work

Fig. 3 Relative deviation of saturated-liquid densities at different compositions from Eq.(1)

Kishizawa et al. [13], ¢ Ikeda and Higashi [9], Widiatmo et al. [7]
Zhelezny et al. [12], This work

Fig. 4 Relative deviation of saturated-liquid densities at different temperatures from Eq.(1)

Kishizawa et al. [13], ¢ Ikeda and Higashi [9], Widiatmo et al. [7]
Zhelezny et al. [12], This work

Fig. 5 Relative deviation of liquid densities at different compositions from Eq.(5)

This work £ Saturated- liquid densities
Compressed- liquid densities
~ Widiatmo et al. [7]

Fig. 6 Relative deviation of liquid densities at different temperatures from Eq.(5)

This work 0 mass % R-125, 20 mass % R-125, 40 mass % R-125
¢ 50 mass % R-125, 60 mass % R-125, £ 80 mass % R-125
¡ 100 mass % R-125
~ Widiatmo et al. [7]

Table I Measured Bubble-Point Pressures and Saturated-Liquid Densities

T (K)	P (MPa)	ρ (kg·m^{-3})	T (K)	P (MPa)	ρ (kg·m^{-3})
x_1= 0 (R-143a)					
249.981	0.281	1097.3	299.986	1.326	919.9
259.984	0.401	1065.4	299.988	1.324	918.9
269.987	0.562	1032.7	309.985	1.702	873.5
279.988	0.764	998.4	309.986	1.700	872.8
279.988	0.762	996.9	319.986	2.149	817.7
289.988	1.015	959.4	319.986	2.150	818.6
289.988	1.017	961.3	329.986	2.689	750.0
x_1 = 0.1461					
279.988	0.764	1047.0	309.986	1.708	916.5
289.988	1.018	1008.3	319.986	2.165	859.5
299.987	1.330	964.8			
x_1 = 0.3181					
279.987	0.765	1098.7	309.986	1.720	962.5
289.987	1.022	1058.6	319.986	2.180	902.5
299.986	1.337	1013.3	329.998	2.732	825.8
x_1 = 0.4110					
279.987	0.768	1125.6	309.986	1.729	985.8
289.987	1.028	1084.4	319.986	2.195	924.1
299.986	1.345	1037.8	329.998	2.749	844.4
x_1 = 0.5163					
279.987	0.773	1158.6	309.986	1.746	1012.9
289.987	1.035	1115.3	319.986	2.215	948.2
299.986	1.356	1067.0	329.998	2.776	863.9
x_1 = 0.7369					
279.987	0.799	1215.4	299.986	1.394	1117.9
289.987	1.067	1169.8	309.986	1.794	1058.9
x_1 = 1 (R-125)					
279.988	0.827	1287.0	309.986	1.858	1112.4
289.988	1.101	1236.4	319.963	2.358	1032.3
299.987	1.443	1179.2			

Table II Measured Compressed-Liquid $P\rho Tx$ Properties

T (K)	P (MPa)	ρ (kg·m^{-3})	T (K)	P (MPa)	ρ (kg·m^{-3})
		x_1 = 0 (R-143a)			
249.981	0.504	1097.9	279.987	2.202	1007.8
249.981	1.001	1099.9	279.988	2.503	1009.7
249.981	1.500	1101.3	279.988	3.007	1013.7
249.981	1.993	1103.0	289.988	1.218	962.9
249.981	2.529	1104.6	289.988	1.501	965.2
249.981	3.006	1106.1	289.989	1.804	967.7
259.984	1.015	1068.4	289.987	2.203	970.8
259.984	1.538	1070.4	289.988	2.603	973.7
259.984	2.014	1072.2	289.987	3.003	976.8
259.984	2.513	1074.1	299.987	1.506	922.1
259.984	3.021	1076.2	299.986	2.002	927.4
269.987	1.031	1035.7	299.987	2.500	932.6
269.987	1.532	1038.0	299.986	3.003	937.2
269.987	2.055	1040.7	309.987	2.003	878.1
269.987	2.524	1043.0	309.986	2.505	885.5
269.987	3.013	1045.2	309.987	3.002	891.8
279.988	1.003	1000.1	319.984	2.510	827.6
279.988	1.303	1002.6	319.985	2.998	837.9
279.988	1.602	1004.3	329.985	3.013	764.0
279.988	1.901	1006.1			
		x_1 =0.1461			
279.988	1.008	1048.8	299.987	2.022	972.6
279.988	1.521	1052.4	299.987	2.520	978.0
279.988	2.067	1056.0	299.987	3.024	983.1
279.988	2.507	1058.9	309.986	2.140	923.6
279.988	3.013	1061.8	309.986	2.507	928.8
289.988	1.564	1013.0	309.986	3.012	936.0
289.988	2.013	1016.8	319.986	2.698	872.4
289.988	2.508	1020.8	319.986	3.013	879.4
289.988	3.027	1024.9			
		x_1 = 0.3181			
279.988	1.076	1100.9	299.987	2.012	1021.5
279.988	1.534	1104.3	299.987	2.505	1027.0
279.988	2.015	1107.7	299.987	3.041	1032.8
279.988	2.533	1111.4	309.986	2.121	969.5
279.988	3.012	1114.6	309.986	2.526	976.1
289.988	1.611	1064.1	309.986	3.043	983.9
289.988	2.009	1067.7	319.986	2.579	913.3
289.988	2.511	1072.0	319.986	3.025	923.8
289.988	3.005	1076.0	329.985	3.033	841.7
299.987	1.526	1015.6			

Table II Measured Compressed-Liquid $P\rho Tx$ Properties (continued)

T (K)	P (MPa)	ρ (kg·m^{-3})	T (K)	P (MPa)	ρ (kg·m^{-3})
		x_1 = 0.4110			
279.988	1.090	1128.5	299.987	2.159	1047.9
279.988	1.512	1131.5	299.987	2.510	1052.1
279.988	2.012	1135.1	299.987	3.011	1057.7
279.988	2.537	1138.8	309.986	2.086	992.3
279.988	3.012	1142.0	309.986	2.522	999.6
289.988	1.542	1089.2	309.986	3.003	1007.2
289.988	2.016	1093.1	319.986	2.773	939.8
289.988	2.508	1097.0	329.985	3.008	859.0
289.988	3.011	1102.4			
		x_1 = 0.5163			
279.988	1.029	1160.2	299.987	2.057	1076.0
279.988	1.554	1164.4	299.987	2.549	1082.0
279.988	2.043	1168.1	299.987	3.005	1087.3
279.988	2.560	1171.6	309.986	2.103	1019.5
279.988	3.040	1175.0	309.986	2.510	1026.6
289.988	1.578	1120.3	309.986	3.012	1034.8
289.988	2.003	1124.6	319.986	2.564	958.7
289.988	2.533	1129.6	319.986	3.010	970.5
289.988	3.004	1133.5	329.985	3.052	880.7
299.987	1.567	1069.7			
		x_1 = 0.7369			
279.988	1.068	1217.2	299.987	2.027	1126.7
279.988	1.523	1221.4	299.987	2.521	1133.1
279.988	2.056	1226.0	299.987	2.998	1139.3
279.988	2.569	1229.7	309.986	2.058	1064.4
279.988	3.045	1233.1	309.986	2.545	1073.6
289.988	1.520	1174.4	309.986	2.957	1081.1
289.988	2.042	1179.5	319.986	2.618	1000.3
289.988	2.502	1184.2	319.986	3.059	1013.1
289.988	3.016	1189.1			
		x_1 = 1 (R-125)			
279.988	1.526	1293.5	289.988	3.025	1257.1
279.988	2.020	1297.7	299.987	2.023	1188.0
279.988	2.519	1301.6	299.987	2.528	1195.7
279.988	3.004	1306.1	299.987	3.039	1202.5
289.988	1.522	1242.0	309.986	2.531	1128.7
289.988	2.011	1246.7	309.986	3.027	1138.5
289.988	2.511	1252.2	319.963	3.012	1056.2

Table III Critical Parameters Used [6]

	R-125	R-143a
T_c (K)	339.17	345.88
P_c (MPa)	3.620	3.764
ρ_c (kg·m^{-3})	577	431
M (g·mol^{-1})	120.02	84.04
w	0.305	0.263
V^* (cm^3·mol^{-1})	208.01	194.99

Table IV Numerical Constants in Eq. 2

	A_m	B_m	C_m	a_m	b_m	c_m
Y_1	0.42700	2.0425	0.57108	3.7043	0.35314	0.85832
Y_2	0.44411	1.7481	0.57467	0.99672	0.42913	0.26212
Y_{12}	-0.027569	-0.35070	-0.029462	-0.91893	-0.093061	-0.45603

Table V Numerical Constants in Eq. (9)

y	y_{ij}		y	y_{ij}		y	y_{ij}	
	d_{11}	0.42711		e_{11}	44.623		f_{11}	0.73408
d_1	d_{12}	0.51492	e_1	e_{12}	33.936	f_1	f_{12}	0.69840
	d_{13}	0.088299		e_{13}	-0.019953		f_{13}	0.013143
	d_{21}	0.21891		e_{21}	331.42		f_{21}	5.6292
d_2	d_{22}	-0.0010140	e_2	e_{22}	317.66	f_2	f_{22}	6.4454
	d_{23}	-0.058131		e_{23}	-0.098548		f_{23}	3.2364
				e_{31}	-0.94528		f_{31}	-0.095887
			e_3	e_{32}	2050.3	f_3	f_{32}	3.3030
				e_{33}	-0.00012525		f_{33}	-1.0378
							f_{41}	13.109
						f_4	f_{42}	13.206
							f_{43}	-0.24057

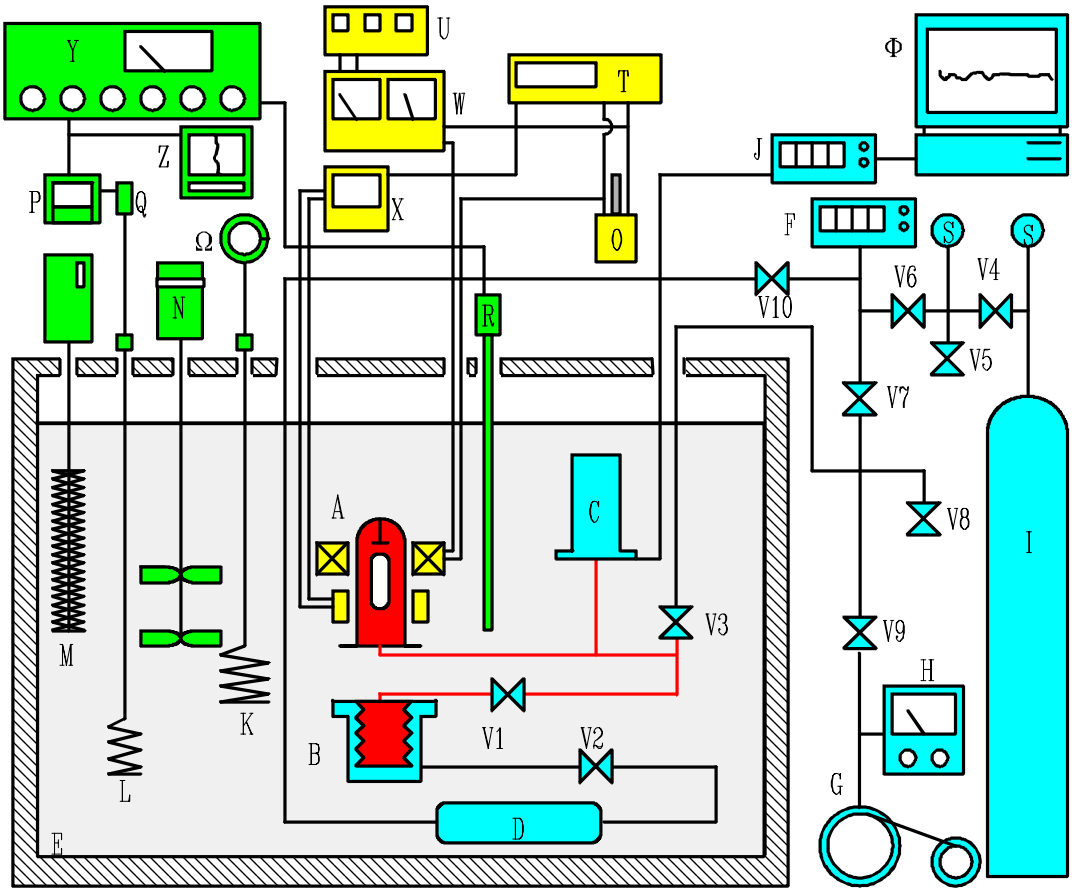

(A) magnetic densimeter (B) variable volume cell (C) digital quartz pressure transducer (D) damper (E) thermostat (F) digital quartz pressure gauge (G) vacuum pump (H) vacuum gauge (I) nitrogen gas (J) digital quartz pressure computer (K) main heater (L) subheater (M) cooler (N) stirrer (O) standard resistor (P) PID controller (R) standard platinum resistance thermometer (S) pressure gauge (T) digital multimeter (U) current controller (V1–V) valves (W) DC power supply (X) galvanometer (Y) thermometer bridge (Z) pen recoder (¶) transformer (‡) personal computer

Fig. 1

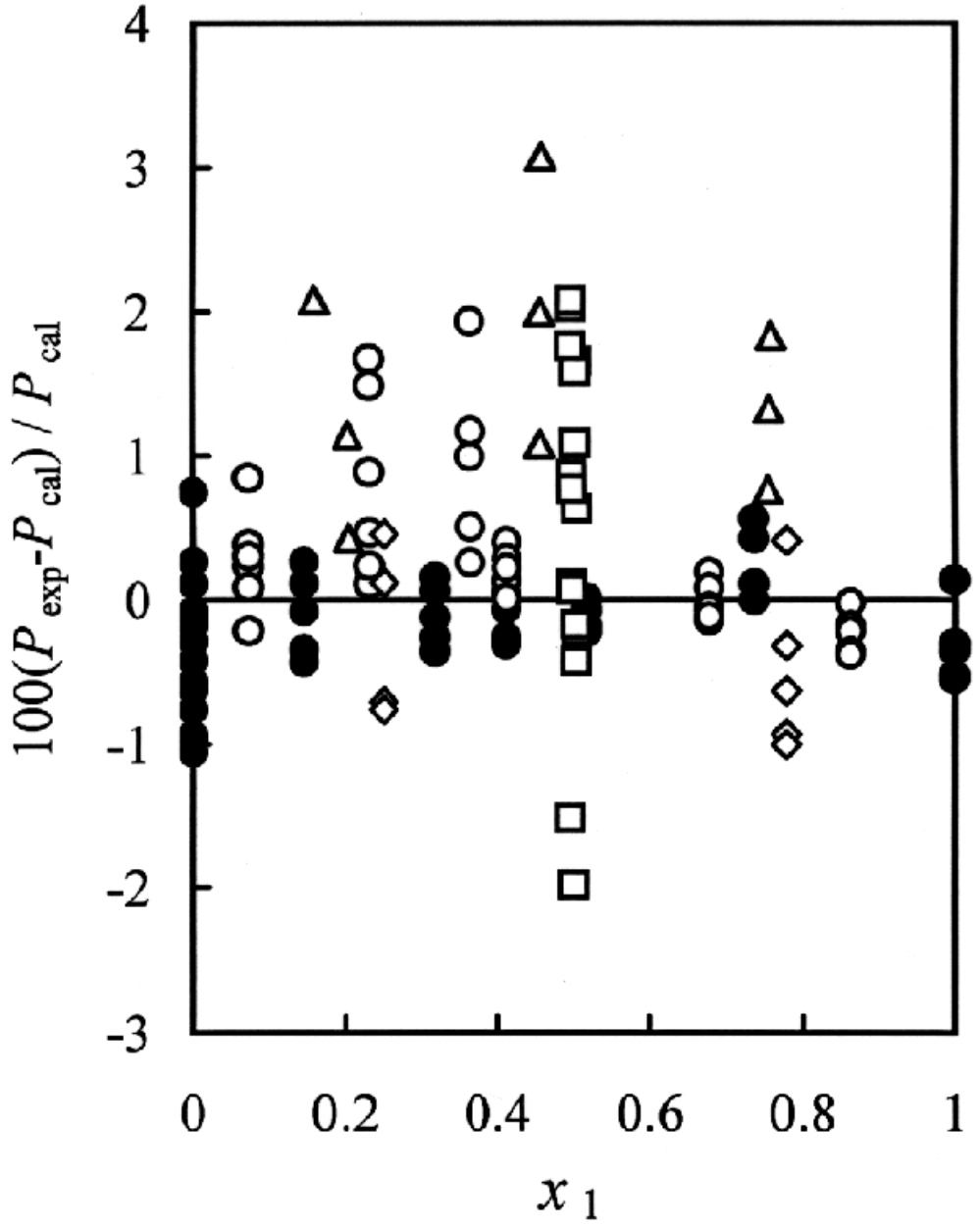

Fig. 2

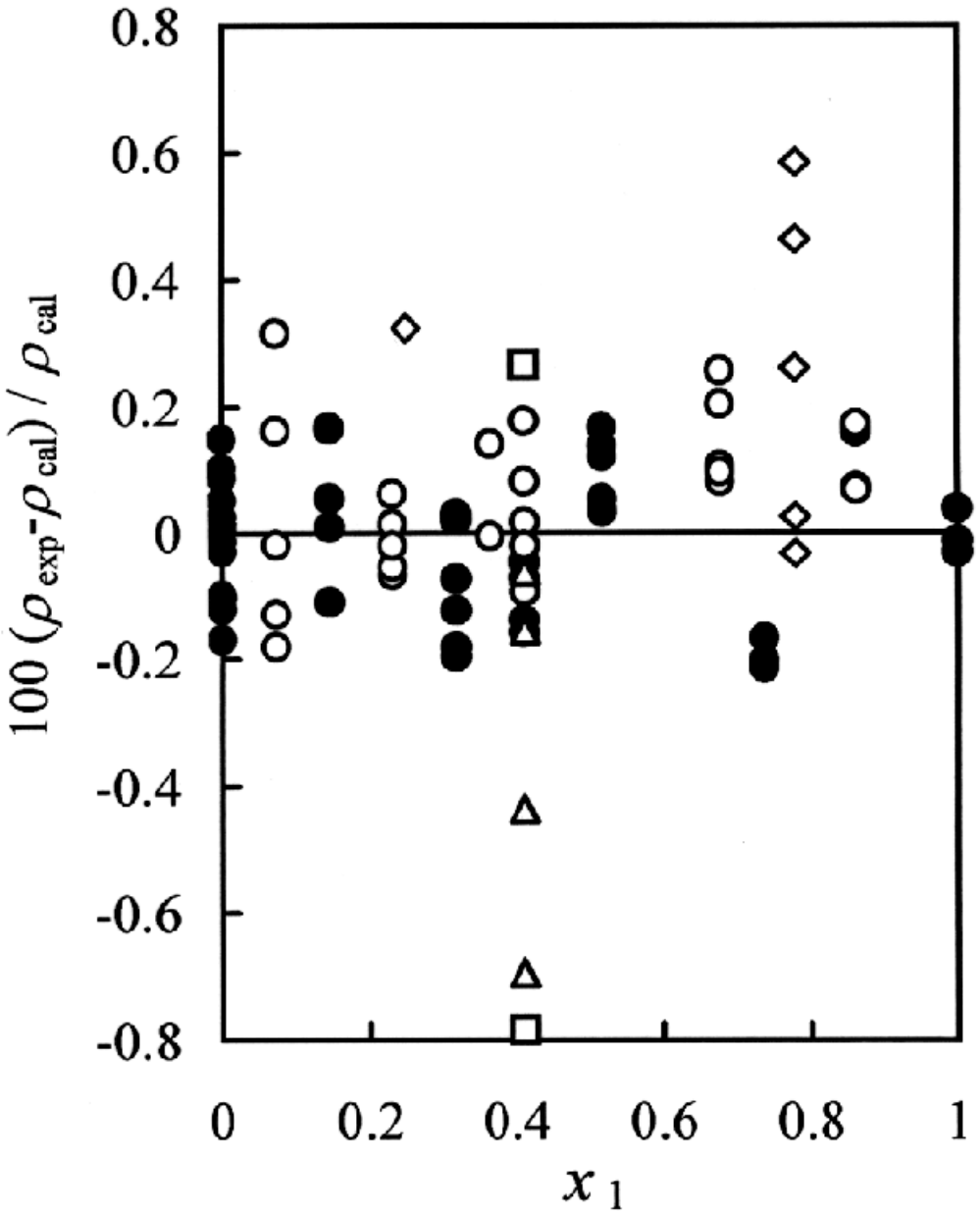

Fig. 3

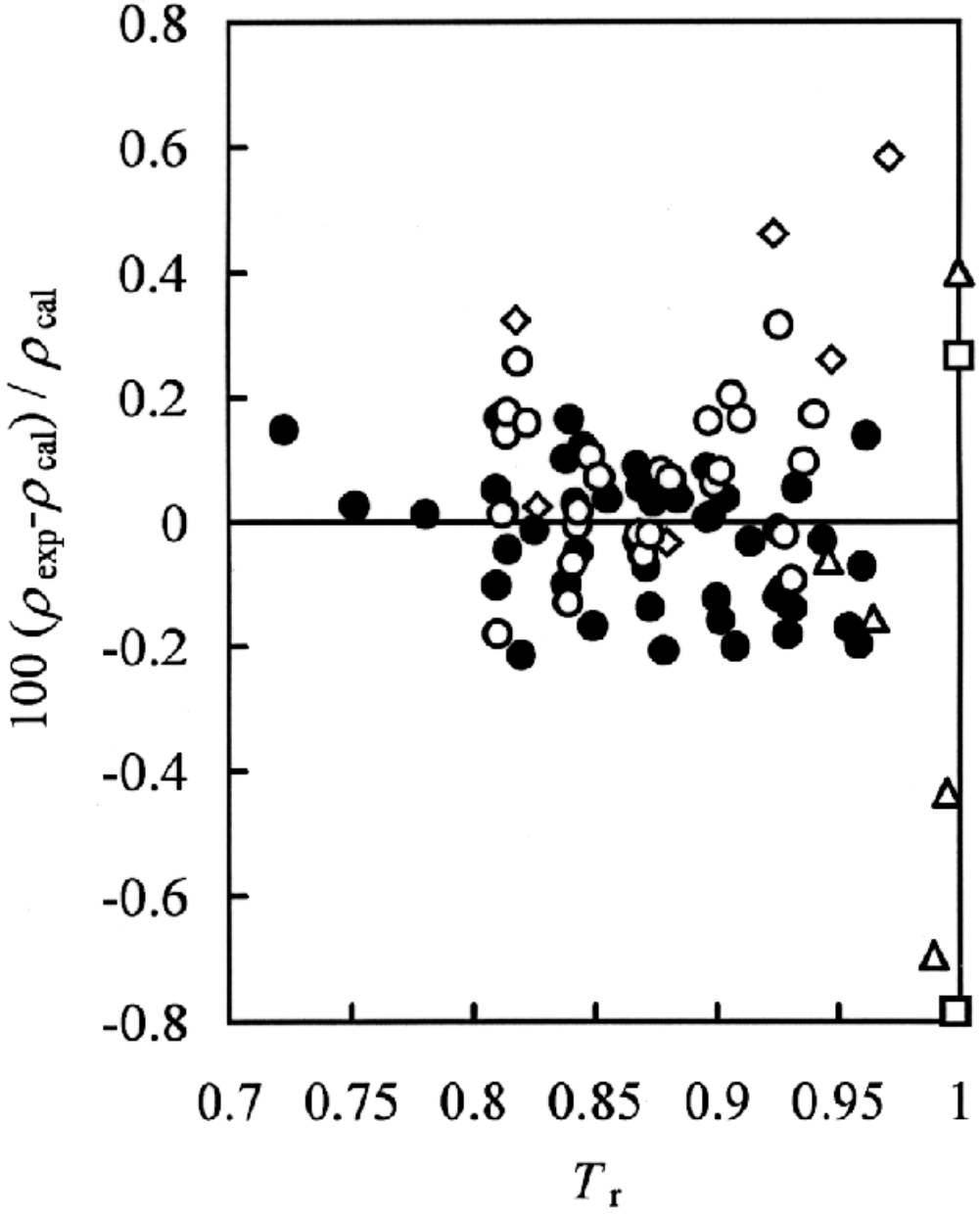
0.8
0.6
0.4
0.2
0
-0.2
-0.4
-0.6
-0.8
100 (ρ exp-ρ cal) / ρ cal
0.7
0.75
0.8
0.85
0.9
0.95
1
T r

Fig. 4

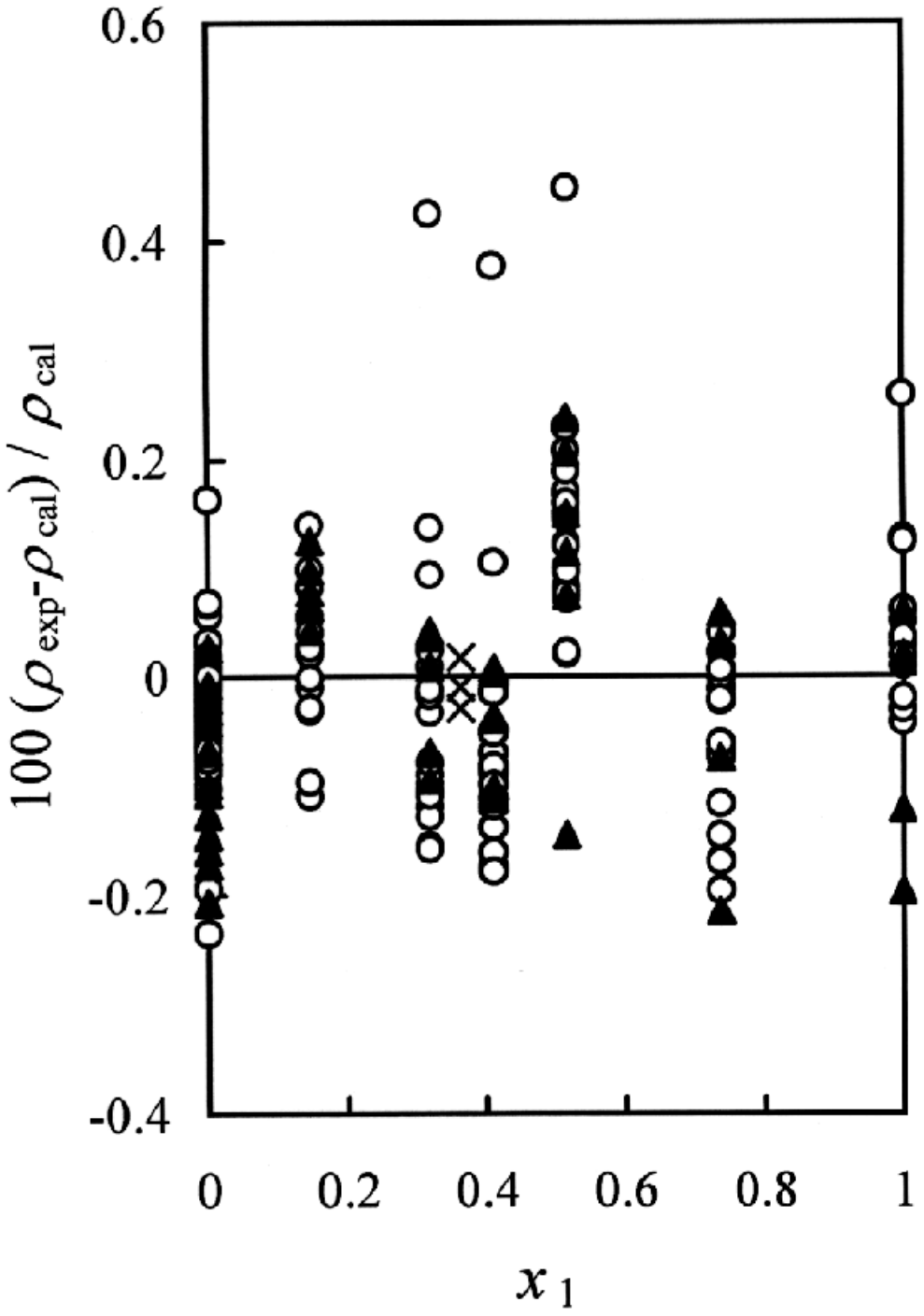

Fig. 5

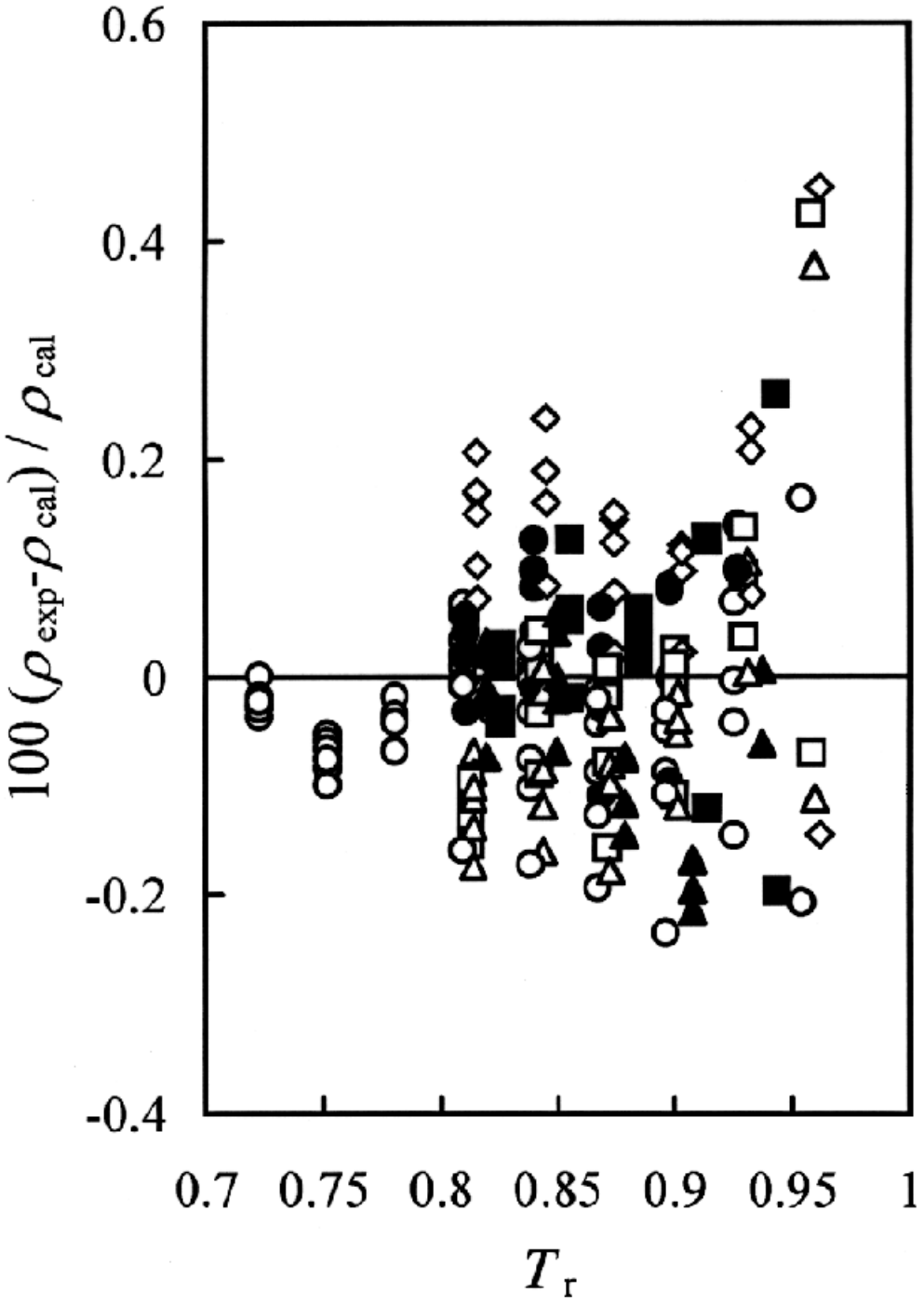

Fig. 6